

Magnetoconductance of thin-film superconductors near critical disorder

W. Brenig

Physik-Department, Technische Universität München, D-8046 Garching, West Germany

M. A. Paalanen and A. F. Hebard

AT&T Bell Laboratories, Murray Hill, New Jersey 07974

P. Wölfle

*Physik-Department, Technische Universität München, D-8046 Garching, West Germany,
and Max-Planck-Institut für Physik und Astrophysik, D-8000 München-40, West Germany*

(Received 21 June 1985)

Gauge-invariant approximations are used to derive all diagrams for the current response function to lowest order in the superconducting pair fluctuations. The resulting expression for the magnetoconductance extends the range in temperature and magnetic field over which meaningful comparisons with experimental data can be made. This aspect of the theory is illustrated in an analysis of magnetoconductance data on 100-Å-thick In/InO_x superconductors near critical disorder where the transition temperature is rapidly suppressed with increasing sheet resistance. The temperature dependence and magnitude of the derived inelastic scattering rate is in good agreement with theory which includes the effect of superconducting fluctuations on the two-dimensional inelastic electron-electron scattering rate.

I. INTRODUCTION

Only recently have theoretical ideas and experimental evidence begun to converge towards a unified understanding of how weak localization and Coulomb interactions affect the resistance of two-dimensional (2D) disordered superconductors. This understanding has been confined primarily to the paraconductivity regime, i.e., the region above the mean-field transition temperature T_{c0} where there is an enhanced conductivity owing to presence of superconducting fluctuations. The early ideas of Maki,¹ Thompson,² and Aslamazov and Larkin³ stimulated an intense and productive period of research into the problem of "fluctuation conductivity." The more recent theoretical treatments,⁴⁻⁷ however, have emphasized the previously ignored contributions of weak localization and Coulomb interactions. In particular, the work by Larkin⁴ demonstrated how the inclusion of impurity vertex corrections to the Maki diagram could lead to a determination of the inelastic electron lifetime τ_i from magnetoconductance (MC) measurements. This seminal work stimulated a number of experiments in which the MC of thin films of Al (Refs. 8-12), Bi_{0.9}Tl_{0.1} (Ref. 12), Sn (Ref. 12), Zn (Ref. 13), W-Re (Ref. 14), and In/InO_x (Ref. 15) have been reported.

Because Larkin's theory is valid only when the inequalities

$$\ln \left(\frac{T}{T_{c0}} \right) \gg \frac{\hbar}{k_B T \tau_i} \quad (1.1)$$

and

$$\ln \left(\frac{T}{T_{c0}} \right) \gg \frac{4eDH}{ck_B T} \quad (1.2)$$

are satisfied (D is the electron diffusivity and H the magnetic field), the experiments are necessarily confined to low fields and temperatures not too close to T_{c0} . In addition, there are complications arising from the Aslamazov-Larkin (AL) contribution to the MC (Refs. 16-18) which dominate near T_{c0} , and the Coulomb contributions¹⁹ in the particle-hole and particle-particle channels, which can be important at higher magnetic fields.

Recently, Lopes dos Santos and Abrahams²⁰ have extended the region of validity of the Larkin result, both in field and in temperature, to the extent that the inequalities (1.1) and (1.2) with $\ln(T/T_{c0})$ replaced by unity have to be satisfied. They have also shown that at high field the superconducting fluctuations are completely suppressed so that the MC saturates at a value $-\sigma(0)$, the negative of the Maki-Thompson conductivity at zero field.^{1,2} The theory presented in the next section (Sec. II) is valid with respect to an even larger range of parameters, limited only by the one condition

$$4 \frac{e}{c} DH \ll \frac{\hbar}{\tau}, \quad (1.3)$$

where τ is the elastic momentum relaxation time. This is the condition for the applicability of a quasiclassical treatment of the magnetic field. The theory contains the above-mentioned results as limiting cases. In addition, a theory of the AL contribution to the MC, valid in the same regime, is presented. It is argued that the Maki-Thompson and AL contribution constitute the dominant terms in a temperature region not too far above T_{c0} . The compact form of the theoretical result facilitates comparison with experiment.

Such a comparison is made in Sec. III, where the dependence of τ_i^{-1} on T and the normal-state resistance R_n is extracted from MC measurements on thin-film

In/InO_x superconducting films near critical disorder where superconductivity is strongly weakened by localization and interaction effects. [Electric-field-effect mobility studies²¹ suggest that critical disorder in thicker (600 Å) films is a result of Anderson localization and occurs when the disorder parameter $k_F l$, the product of the Fermi wave vector and the elastic scattering mean free path, is on the order of $\sqrt{3}$.] The magnitude of τ_i^{-1} is found to be slightly less than the upper bound determined by the energy gap and to have an approximately linear temperature dependence. Good qualitative agreement with a recently published theory,²² which includes the additional inelastic process of the single electrons recombining into Cooper pairs, is also obtained.

II. THEORY

The transition to a superconducting state, in which pairs of electrons are correlated, is signaled by the appearance of a pole in the scattering amplitude for two electrons with equal but opposite momenta. In a perturbation theoretical calculation terms involving the pair vertex function (or fluctuation propagator) are therefore strongly enhanced. Near, but not too close to, the transition temperature T_{c0} it is sufficient to consider only contributions with one or two fluctuation propagators.¹⁻³

In a dirty metal, the superconducting fluctuations are strongly perturbed by elastic scattering of the electrons

$$K(q, \omega_l) = -N_0^{-1} \left[-\frac{1}{g(T)} + \psi\left(\frac{1}{2} + (|\omega_l| + Dq^2 + 1/\tau_i)/4\pi T\right) - \psi\left(\frac{1}{2}\right) \right]^{-1}, \quad (2.3)$$

where a temperature-dependent coupling constant is defined by

$$\frac{1}{g(T)} = \frac{1}{N_0 V_0} + \ln \left[\frac{2\gamma \epsilon_c}{\pi T} \right] \quad (2.4)$$

and N_0 is the density of states at the Fermi level for one spin species. For a superconducting system V_0 is negative and the cutoff energy ϵ_c is of the order of the Debye energy (γ is Euler's constant). Then g may be expressed in terms of the (unrenormalized) transition temperature T_{c0}^0 as $g^{-1} = \ln(T_{c0}^0/T)$.

The effect of a weak perpendicular magnetic field H on the orbital motion of the electrons may be treated in the quasiclassical approximation. This amounts essentially to replacing Dq^2 by the Landau quantized energy levels $a(j + \frac{1}{2})$, where $a = 4eDH$. At the same time the sum on q has to be replaced by the sum on j ($j = 0, 1, 2, \dots$) multiplied by the degeneracy factor (eH/π).

It is worth noting that the pole of the fluctuation propagator for $\omega_l = 0$ is shifted by the inelastic scattering rate $1/\tau_i$ as well as by a magnetic field, which both act as pair-breaking sources. In zero magnetic field, the shifted (mean-field) transition temperature T_{c0} is obtained from the zero of the denominator in (2.3) as

$$\ln \left[\frac{T_{c0}}{T_{c0}^0} \right] = \psi\left(\frac{1}{2}\right) - \psi\left(\frac{1}{2} + 1/4\pi T_{c0} \tau_i\right). \quad (2.5)$$

from static impurities. The fluctuation propagator may then be taken to satisfy the equation

$$K(q, \omega_l) = V_0 - V_0 T \sum_{\epsilon_n} \sum_{\mathbf{p}} [C(\epsilon_n + \omega_l, \epsilon_n; q) G_{\mathbf{p}+\mathbf{q}}(\epsilon_n + \omega_l) \times G_{-\mathbf{p}}(-\epsilon_n)] K(q, \omega_l), \quad (2.1)$$

where V_0 represents the interaction. We assume the photon-mediated interaction to dominate the Coulomb interaction, which justifies the omission of any frequency and momentum dependence from the interaction function V_0 . The particle-particle impurity ladder $C(\epsilon_n, \epsilon'_n; q)$ (Cooperon) is given by

$$C(\epsilon_n, \epsilon'_n; q) = \frac{1}{\tau} \frac{1}{|\epsilon_n - \epsilon'_n| + Dq^2 + 1/\tau_i} \times \Theta(-\epsilon_n \epsilon'_n) + \Theta(\epsilon_n \epsilon'_n) \quad (2.2)$$

with τ the elastic relaxation time and $D = \frac{1}{2} v_F^2 \tau$ the bare diffusion constant (Θ is the step function). Here, we take into account inelastic processes, destroying the phase coherence of the Cooperon, by adding an inelastic relaxation rate $1/\tau_i$. Later we shall calculate τ_i .

With these approximations, the fluctuation propagator is easily calculated in terms of the digamma function ψ , as¹ ($\mathcal{K}_1 k_3 = 1$)

As a guiding principle in formulating a systematic approximation it is useful to require gauge invariance of the theory.²³ A gauge-invariant approximation may be constructed by starting from a set of closed diagrams. We choose the diagram that may be formed by closing a particle-particle (pp) ladder consisting of an arbitrary series of interaction and impurity lines on itself as our starting set (Fig. 1). The single-particle propagators are understood to be impurity averaged in the sense of the self-consistent Born approximation (SCBA). The approximation for the self-energy and the vertex function, is obtained by cutting a single (bare) Green's-function line or two G lines, respectively. In this way we find for the self-energy the approximation shown in Fig. 2. For the vertex function, or equivalently, the current-correlation function the diagrams depicted in Fig. 3 are generated. Here Fig. 3(a) is the so-called Maki diagram and Figs. 3(b) and 3(b') represent the Aslamazov-Larkin diagrams. We have not explicitly shown the self-energy contributions, because they are less singular than Figs. 3(a) and 3(b) and 3(b') near T_{c0} and will be neglected. A complete derivation of all these terms will be given elsewhere.²⁴

We have evaluated (for details of the derivation see Ref. 24) the contributions to the magnetoconductivity shown in Fig. 3 assuming the temperature T and the pair-breaking fields $a, 1/\tau_i$ to be small compared to the elastic rate $1/\tau$, but otherwise arbitrary. The result for the total Maki-Larkin contribution [Fig. 3(a)] is obtained as

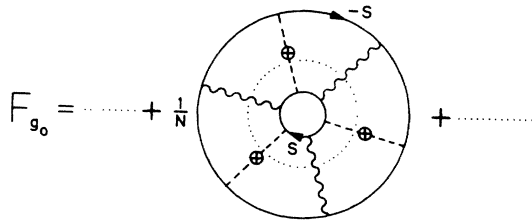


FIG. 1. Vacuum diagrams composed of a single particle-particle ladder with alternating (dashed-crossed) impurity lines and (wiggly) interaction lines. s denotes the spin.

$$\sigma_{ML} = \frac{e^2}{2\pi^2} \frac{a}{4\pi T} \sum_{l=0}^{\infty} \frac{1}{\eta_l} \beta(g, \eta_l), \quad (2.6)$$

where

$$\beta(g, \eta_l) = -2\pi \int_{-\infty}^{\infty} dx \frac{1}{\sinh^2(2\pi x)} [\text{Im}\Gamma_l(ix)] \times [\text{Im}\psi(\frac{1}{2} + \eta_l + ix)] \quad (2.7)$$

and

$$\eta_l = \frac{a(l + \frac{1}{2}) + 1/\tau_l}{4\pi T}. \quad (2.8)$$

$$\beta(T, \eta_l) = \frac{1}{2} \left\{ \psi'(\frac{1}{2} + \eta_l) \Gamma_l(0) + \sum_{k(\geq 1)} \left[\left[\frac{\pi^2}{\cos^2[\pi(\frac{1}{2}k + \eta_l)]} + \psi'(\frac{1}{2} + \eta_l + \frac{1}{2}k) - \psi'(\frac{1}{2} - \eta_l + \frac{1}{2}k) \right] \Gamma_l(\frac{1}{2}k) - \{ \pi \tan[\pi(\frac{1}{2}k + \eta_l)] + \psi(\frac{1}{2} - \eta_l + \frac{1}{2}k) - \psi(\frac{1}{2} + \eta_l + \frac{1}{2}k) \} \Gamma_l'(\frac{1}{2}k) + \left[\frac{(-1)^k - 1}{2} \right] \frac{4\pi^2}{\sin^2(2\pi\eta_l)} \Gamma_l(\frac{1}{2}k + \eta_l) \right] \right\}. \quad (2.10)$$

However, the integral representation (2.7) is more amenable to numerical evaluation because of the slow convergence of the sum in (2.10). A useful approximation (accurate to about 10%) results from expanding the factor multiplying $\sinh^{-2}(2\pi x)$ in the integrand of (2.7) in the numerator and denominator to first order in x . The integral can then be done analytically:

$$\beta \cong 4R_l \psi'(2R_l) - \frac{1}{2R_l} - 2, \quad (2.11)$$

where

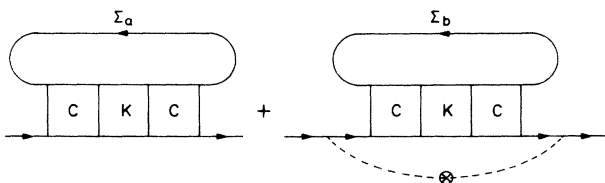


FIG. 2. Self-energy diagrams in first order in the pair fluctuation propagator K .

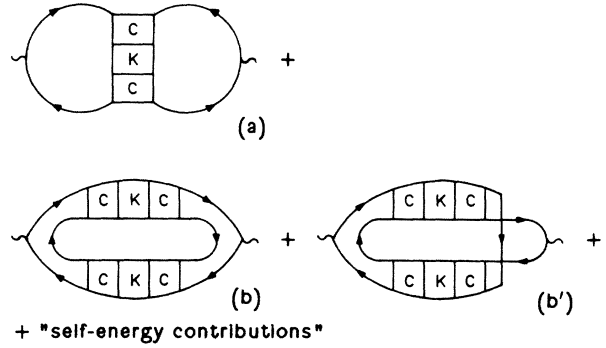


FIG. 3. Diagrams of the current response function, obtained by attaching two current vertices to the diagrams of Fig. 1.

Here ψ is the digamma function and Γ_l is defined by

$$\Gamma_l(z) = \frac{1}{-\frac{1}{g} + \psi(\frac{1}{2} + \eta_l + z) - \psi(\frac{1}{2})}. \quad (2.9)$$

The integral in (2.7) may be converted into a sum over residues:

$$R_l = \left[-\frac{1}{g} + \psi(\frac{1}{2} + \eta_l) - \psi(\frac{1}{2}) \right] / \psi'(\frac{1}{2} + \eta_l). \quad (2.12)$$

Close to the transition, when $|g^{-1}| \rightarrow 0$, and for $a, 1/\tau_l \ll T$, and hence $\eta_l \rightarrow 0$, one finds

$$\beta_l \cong \frac{2\pi T}{a(l + \frac{1}{2}) + 1/\tau_{GL}}, \quad (2.13)$$

where

$$1/\tau_{GL} = (8T/\pi) \ln(T/T_{c0}) \quad (2.14)$$

defines the Ginzburg-Landau time. When this is substituted into (2.6) and the l sum is performed, the following result for the magnetoconductance is obtained

$$\sigma_{ML} \cong \frac{e^2}{\pi} \frac{T}{\tau_{GL}^{-1} - \tau_l^{-1}} [\psi(\frac{1}{2} + 1/a\tau_{GL}) - \psi(\frac{1}{2} + 1/a\tau_l)]. \quad (2.15)$$

In the limit of zero magnetic field this reduces to the well-known result²

$$\sigma_{\text{ML}}(H=0) = \frac{e^2}{\pi} \frac{T}{1/\tau_{\text{GL}} - 1/\tau_i} \ln(\tau_i / \tau_{\text{GL}}). \quad (2.16)$$

In the limit $\eta_l \ll \ln(T/T_{c0})$ the dependence of β_l on η_l may be neglected altogether and

$$\beta = \frac{\pi^2}{4} \sum_k (-1)^k \Gamma(|\frac{1}{2}k|) - \frac{1}{4} \sum_{k(\geq 0)} \Gamma''(\frac{1}{2}(2k+1)), \quad (2.17)$$

where $\Gamma(z) = \Gamma_l(z)$ and $\Gamma''(z) = d^2\Gamma_l(z)/d\eta_l^2$ at $\eta_l=0$, in agreement with the result by Larkin⁴ [Note the factor of 2 difference in the frequency argument in Larkin's definition of Γ . Also, in his Eq. (7) the term $\Gamma(|m|)$ should be multiplied by the step function $\Theta(m)$ and the sign in front of sign (m) should be reversed.] The result of Lopes dos Santos and Abrahams²⁰ follows from the general result (2.7) by expanding Γ_l^{-1} in first order in η_l and neglecting η_l in the argument of $\text{Im}\psi$.

In Fig. 4 we compare the results of a numerical evaluation of σ_{ML} as given by the exact expressions (2.6) and (2.7) (solid lines), the approximate expression (2.15) (dashed lines), and the expression (2.17) (dashed-dotted lines) as a function of magnetic field for typical values of temperature and $\gamma_i = (2\pi T\tau_i)^{-1}$. Larkin's result (2.17) is seen to agree with the exact result [Eqs. (2.6) and (2.7)] for temperatures sufficiently far above T_{c0} , small inelastic scattering rate, i.e., $\tau_i \gg \tau_{\text{GL}}$, and not too high magnetic fields. At high magnetic fields, $a \gg \tau_{\text{GL}}^{-1}$, the fluctuation contribution to the conductivity is completely suppressed. This is not correctly described by (2.17), because of the neglect of a cutoff in the sum over l .

In Fig. 5 the temperature dependence of the fluctuation-induced conductivity as obtained by evaluating the exact result [(2.6) and (2.7)] and the Maki-Thompson result (2.16) is shown for zero magnetic field and $\gamma_i(T_c) = 0.1$.

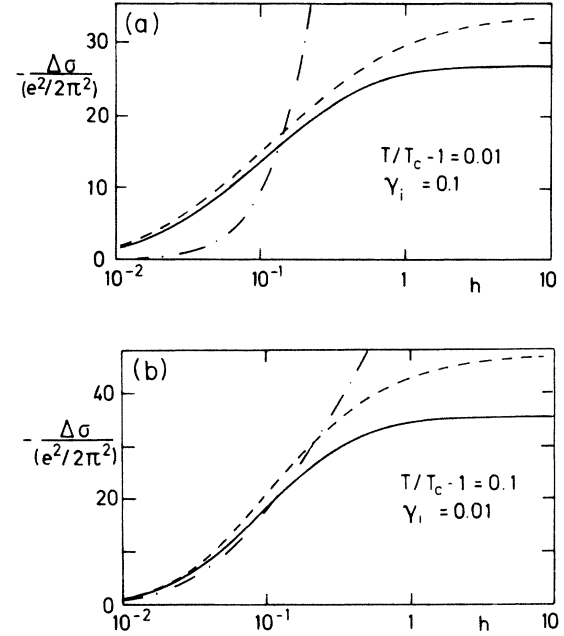


FIG. 4. Maki-Larkin contribution to the magnetoconductance $-\Delta\sigma/(e^2/2\pi^2)$ versus magnetic field $h = 2DeH/\pi T$ for typical values of $\gamma_i = 1/(2\pi T\tau_i)$ and temperature.

The Aslamazov-Larkin contribution given by Figs. 3(b) and 3(b') may be calculated along similar lines. The result is

$$\sigma_{\text{AL}} = \frac{e^2}{2\pi^2} \sum_{l=0}^{\infty} (l+1) \delta_l(g, \eta_l, \eta_{l+1}), \quad (2.18)$$

where the function δ_l is defined by

$$\begin{aligned} \delta_l = & \int dx \frac{2\pi}{\sinh^2(2\pi x)} (\text{Re}[\Gamma_{l+1}(-ix)\Gamma_l(ix)] \{ \text{Re}[\psi(\frac{1}{2}-ix+\eta_{l+1})-\psi(\frac{1}{2}-ix+\eta_l)] \}^2 \\ & - \text{Re}\{\Gamma_{l+1}(-ix)\Gamma_l(-ix)[\psi(\frac{1}{2}-ix+\eta_{l+1})-\psi(\frac{1}{2}-ix+\eta_l)]^2\}) \\ & - \int dx \coth(2\pi x) \text{Re}\{\Gamma_{l+1}(-ix)\Gamma_l(-ix) \frac{\partial}{\partial x} [\psi(\frac{1}{2}-ix+\eta_{l+1})-\psi(\frac{1}{2}-ix+\eta_l)]^2\}. \end{aligned} \quad (2.19)$$

In this case it is not possible to do the first of the integrals in (2.19) analytically, because the arguments of the two-pair propagators in the product are on different sides of the real axis. The second integral, however, may be converted into a reasonably fast converging sum.

Employing again the approximation of expanding the expression within bold parentheses in the first integral to first order in x the following result is obtained:

$$\begin{aligned} \delta_l = & \frac{4\phi_l(\phi_l - \phi'_l(R_{l+1} + R_l))}{\psi'(\frac{1}{2} + \eta_{l+1})\psi'(\frac{1}{2} + \eta_l)(R_{l+1} + R_l)} \left[\frac{2R_l\psi'(2R_l) - 2R_{l+1}\psi'(2R_{l+1})}{R_{l+1} - R_l} - \frac{1}{4R_{l+1}R_l} \right] \\ & + 2 \sum_{k(\geq 1)} [\Gamma_{l+1}(\frac{1}{2}k) - \Gamma_l(\frac{1}{2}k)] [\psi'(\frac{1}{2} + \frac{1}{2}k + \eta_{l+1}) - \psi'(\frac{1}{2} + \frac{1}{2}k + \eta_l)] + [\Gamma_{l+1}(0) - \Gamma_l(0)] \phi'_l. \end{aligned} \quad (2.20)$$

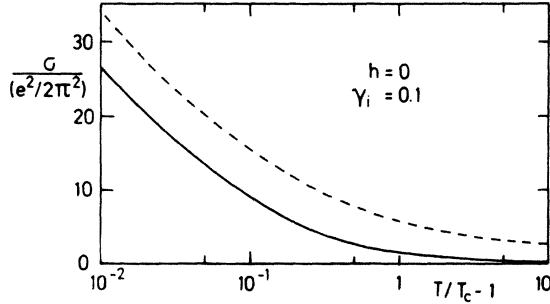


FIG. 5. Maki-Larkin contribution to the zero-field conductance versus temperature for an inelastic scattering rate given by $\gamma_i = 1/2\pi T\tau_i = 0.1$. The exact result (solid line) according to Eqs. (2.6) and (2.7) is compared with the Maki-Thompson result (2.16) (dashed line).

Here the abbreviations

$$\phi_l = \psi\left(\frac{1}{2} + \eta_{l+1}\right) - \psi\left(\frac{1}{2} + \eta_l\right), \quad (2.21)$$

$$\phi'_l = \psi'\left(\frac{1}{2} + \eta_{l+1}\right) - \psi'\left(\frac{1}{2} + \eta_l\right) \quad (2.21')$$

have been used, and R_l is defined by (2.12).

In the limit $T \rightarrow T_{c0}$, and for $\eta_l \ll 1$, one may put $\phi_l = \pi a/8T$. Making use of $R_l \ll 1$ and

$$[\psi'(\frac{1}{2} + \eta_l)R_l]^{-1} \gg \Gamma_l(\frac{1}{2}k)$$

for $k \neq 0$, in (2.20) one obtains

$$\delta_l = \frac{2\pi T}{a} \left[\left[l + \frac{1}{2} + \frac{1}{a\tau_{GL}} \right] \left[l + 1 + \frac{1}{a\tau_{GL}} \right] \times \left[l + \frac{3}{2} + \frac{1}{a\tau_{GL}} \right] \right]^{-1}. \quad (2.22)$$

By substituting (2.22) into (2.18), the Aslamazov-Larkin contribution can be cast into the form

$$\sigma_{AL}(h) = \frac{e^2}{2\pi^2} \frac{4\pi T}{a} \left\{ 1 - 2 \frac{1}{a\tau_{GL}} \left[\psi \left[1 + \frac{1}{a\tau_{GL}} \right] - \psi \left[\frac{1}{2} + \frac{1}{a\tau_{GL}} \right] \right] \right\}, \quad (2.23)$$

a result first obtained by Usadel.¹⁶ In the limit of vanishing magnetic field this reduces to the well-known expression³

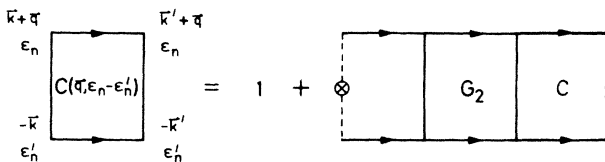


FIG. 6. Integral equation for the impurity particle-particle vertex C (Cooperon).

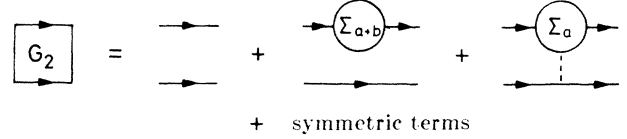


FIG. 7. Diagrams contributing to the irreducible part of the particle-particle propagator G_2 . The dashed line being the Diffusion starting off with one impurity line.

$$\sigma_{AL}(0) = \frac{e^2}{16} \frac{T_c}{T - T_c}. \quad (2.24)$$

The inelastic scattering rate caused by the Coulomb interaction has been calculated by Schmid,²⁵ Abrahams *et al.*,²⁶ Fukuyama and Abrahams²⁷ and Altschuler *et al.*,²⁸ using different methods. The calculation of Ref. 27 may be readily generalized to include pair fluctuation effects originating from the electron-phonon interaction. This is done by incorporating electron interaction effects into the impurity particle-particle propagator C as shown in Fig. 6. Here G_2 is the irreducible part of the particle-particle propagator. Contrary to the treatment by Fukuyama and Abrahams,²⁷ here particle-particle-interaction ladder diagrams are not included in C by definition. We approximate G_2 by the sum of all self-energy diagrams in first order in the pair fluctuations, dressed by all possible impurity vertex corrections. This is shown in Fig. 7, where Σ are the self-energy diagrams shown in Fig. 2. In this approximation the inelastic scattering rate is directly given by the sum of the self-energy terms in Fig. 7. In zero magnetic field the inelastic relaxation rate obtained by evaluating the diagrams of Fig. 7 and adding the Coulomb interaction contribution τ_i^c , is given by the self-consistent equation (for a detailed derivation see Ref. 22)

$$\frac{1}{\tau_i} = \frac{8}{\pi} \frac{T^2}{\epsilon_F \tau} \frac{\tau_i}{1 - \tau_i/\tau_{GL}} \left\{ \frac{1}{1 - \tau_{GL}/\tau_i} \ln \left[\frac{1}{2} (1 + \tau_{GL}/\tau_i) \right] + \frac{1}{1 + \tau_i/\tau_{GL}} \right\} + \frac{1}{\tau_i^c}. \quad (2.25)$$

The initial increase of τ_i^{-1} proportional to $[\ln(T/T_c)]^{-1}$ far above T_{c0} ($\tau_{GL} \ll \tau_i$) is cutoff in the temperature regime where $\tau_{GL} \gtrsim \tau_i$. The enhancement over the Coulomb rate is larger for larger τ , i.e., for weaker disorder. A simple interpolation formula for $1/\tau_i$ is given in Eq. (4.2). The fluctuation contribution to $1/\tau_i$ is suppressed by a magnetic field.²²

III. EXPERIMENT

The films for this study were prepared using the technique of reactive ion-beam sputter deposition in which a constant partial pressure of oxygen is maintained during the sputtering of an indium target with argon ions. All of the films had the same 100 Å thickness and the desired room-temperature resistivity was obtained by carefully chosen deposition parameters: e.g., ion-beam voltage and

current density, deposition rate, and reactive gas pressure. The microstructure of these films has been previously determined by transmission electron microscopy to consist of occasional islands of crystalline In_2O_3 embedded in an amorphous background of In stabilized with oxygen impurities.²⁹ Annealing at $\sim 100^\circ\text{C}$ has been found in earlier work³⁰ to give rise to small decreases in resistance and was used here to make adjustments ($\leq 5\%$) in the resistivity of some of our films.

Figure 8 is a plot on logarithmic axes of the resistive transitions of four films which have room-temperature sheet resistances R_n which increase monotonically from 2248 Ω/\square for film a to 4580 Ω/\square for film d. The mean-field transition temperature T_{c0} for films a–c was determined using Aslamazov-Larkin theory with a procedure described previously.^{30,31} The resulting best-fit temperatures are shown as vertical arrows for the three films which become superconducting at low temperature. The prominent aspect of these data, which has been previously emphasized,¹⁵ is the rapid decrease in T_{c0} for small increases in R_n near critical disorder where R_n has a value on the order of $\hbar/e^2 = 4114 \Omega/\square$. It should be noted that this pronounced sensitivity to the normal-state resistivity does not occur, for example, in three-dimensional (3D) granular aluminum films where the decrease in T_{c0} spans a two to three decade change in resistivity.^{32,33}

Because the superconductivity in our thin In/ InO_x films is so sensitive to the value of R_n , it is important to assess the role of spatially varying inhomogeneities. Our confidence in the homogeneity of our samples is based on the following observations. (1) Day-to-day variations in R_n for a given set of deposition parameters is on the order of 15%. By contrast, the variations for granular aluminum with similar R_n are on the order of a factor of 5. (2) The variation in R_n for adjacent 100 μm wide by 400 μm long strips fabricated on the same substrate is typically $\sim 0.1\%$. The corresponding resistance transitions for

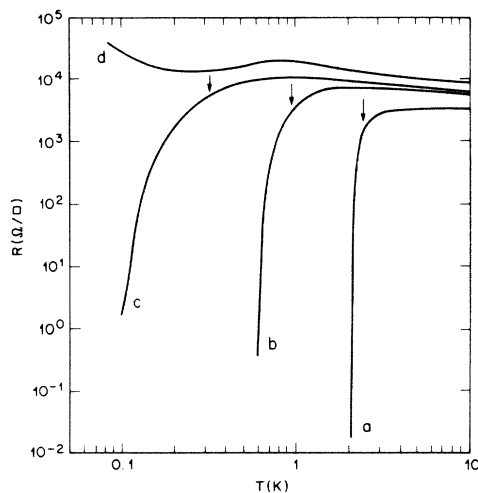


FIG. 8. Logarithmic plot of resistive transitions of four 100-Å-thick In/ InO_x composite films. The transition temperatures, indicated by arrows, are 2.494, 0.973, and 0.326 K for films a–c, respectively.

pairs of these adjacent strips essentially overlap for all but the lowest T_{c0} films (i.e., film c). (3) For the superconducting films there are no bumps or kinks which typically reflect the presence of clusters³⁴ or other large-scale inhomogeneities. (4) Earlier work^{30,35} on the vortex fluctuation regime of similar films with $T_{c0} \geq 2$ K was consistent with Kosterlitz-Thouless predictions³⁶ and confirmed vortex interactions occurring on length scales approaching 100 μm . Such behavior has not been seen in inhomogeneous films.³⁷

The magnetoconductance (MC) data were taken in a dilution refrigerator using a four-terminal resistance bridge operating at frequencies as low as 5 Hz. All measurements were taken at currents sufficiently low to ensure the linearity of voltage with respect to current. Typical magnetoconductance data, defined as the difference $\sigma(H) - \sigma(0)$ normalized to $e^2/2\pi^2\hbar$, is plotted in Fig. 9 against the logarithm of field for film a (squares) at 3.120 K and for film c (triangles) at 0.499 K. To obtain a meaningful comparison with the theory of the preceding section, we have excluded all data in the field regime where the MC has reached saturation and begun to decline. This maximum in the MC is observed only for film c at temperatures less than ~ 2 K and fields $H \geq 30$ kOe. The maximum attainable field of 85 kOe was insufficient to reach saturation of the MC of films a and b.

For a comparison with theory we have opted to use the exact expressions of Eqs. (2.6) and (2.7). This decision was motivated primarily by the rather large errors introduced when the approximate expression of Eq. (2.15) is used at high temperatures and fields (Fig. 4, dashed line). The analysis is performed in terms of the characteristic field

$$H_i = \frac{\hbar c}{4eD\tau_i}, \quad (3.1)$$

which is that field where the magnetic length is roughly

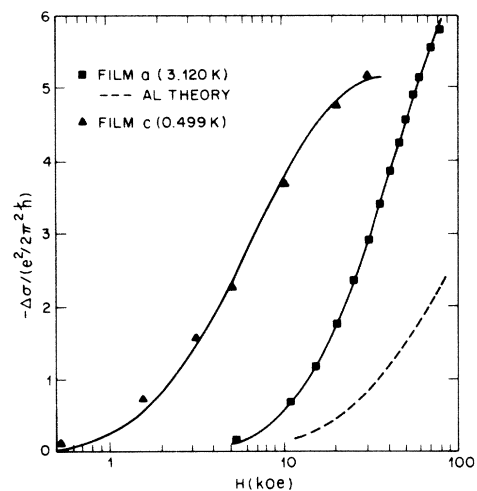


FIG. 9. The negative of the normalized magnetoconductance plotted as a function of field for film a (squares) at 3.120 K and film b (triangles) at 0.499 K. The solid lines are theoretical fits and the dashed line is the Aslamazov-Larkin contribution for film a.

equal to the inelastic diffusion length $L_i = (D\tau_i)^{1/2}$, where τ_i is the electron scattering time and D is the electron diffusivity. The fundamental constants \hbar , k_B , and c are restored in all expressions for the remainder of this discussion. With this notation, the parameters a , τ_i^{-1} , and η_l of Eqs. (2.6), (2.7), and (2.8) become, respectively, $4eDH_i/\hbar c$, $4eDH_i/\hbar c$ and $[a(l + \frac{1}{2}) + \tau_i^{-1}]\hbar/4k_B T\pi$. The transition temperature T_{c0} is included by using Eq. (2.5) in Eq. (2.9). Finally, the effect of weak localization on the normal-state conductivity is taken into account with an additive term due to Hikami *et al.*³⁸ This term is also dependent on D and H_i in addition to an unknown characteristic field $H_{s.o.}$ which is related to the spin-orbit scattering time in the same way that H_i is related to τ_i in Eq. (3.1) above. Spin-flip scattering has been ignored.

From the above discussion we see that there are four input parameters: T_{c0} , D , H_i , and $H_{s.o.}$. The first of these, the mean-field transition temperature T_{c0} , has been measured as discussed above, and the second, the electron diffusivity D , is extracted from critical field H_{c2} measurements. This determination of D is somewhat complicated by our previously published observation¹⁵ that the critical field slopes near T_{c0} decrease with increasing disorder (i.e., decreasing T_{c0}). Within the context of the dirty limit formula, this result implies the unphysical result that D increases with increasing disorder. These problems were circumvented¹⁵ with the *ad hoc* use of a temperature-independent pair-breaking rate in a pair-breaking model. A good fit to the dependences of T_{c0} and $H_{c2}(T)$ on the disorder as measured by R_n was obtained using the value $D=0.18 \text{ cm}^2\text{sec}^{-1}$ for films with T_{c0} in the range 1.0–2.5 K. We use the same value for the films discussed here.

The remaining input parameters, H_i and $H_{s.o.}$, are the unknown fitting parameters which must be varied to obtain a best fit of the theory to the data in a least-squares sense. The most computationally intensive part of this procedure arises from the slow convergence of the summation in Eq. (2.6) for small a , or equivalently, for small H . For the high-temperature data where small values of the MC (≈ 0.01) were typical, “zero” fields as low as 10–20 Oe and summation of as many as 2×10^4 terms were required to obtain sufficient precision in the evaluation of $\Delta\sigma = \sigma(H) - \sigma(0)$. The solid lines in Fig. 9 represent the typical quality of fit which was obtained over the entire range of T and H discussed here.

Ideally one would like to include the Aslamazov-Larkin (AL) contribution to the MC as an additional term. We are reluctant to do this, however, because of the established presence of vortex fluctuations in these films which cause $\sigma(H=0)$ to diverge at the vortex-antivortex unbinding temperature T_c , a temperature which for films with sufficiently high R_n can be significantly below T_{c0} .³⁶ The theoretical expression for the AL contribution to MC (Refs. 16–18) does not take vortex fluctuations into account and consequently diverges at T_{c0} , a temperature where there is still a significant amount of resistance in the sample. There is at present very little understanding of this transition region separating the vortex fluctuation regime from the paraconductivity regime. Accordingly, our expectations are confirmed and the theoretical AL

contribution to the MC is found to diverge much more rapidly than does the experimental MC as $T \rightarrow T_{c0}$. Because of these uncertainties we have chosen to analyze our data only for those temperatures where the AL term can be ignored. The data shown in Fig. 9, for example, are taken for films a and c at temperatures where the AL contribution (dashed line for film a) is beginning to become significant. At higher T the relative importance of this contribution becomes negligibly small.

IV. DISCUSSION

The best-fit temperature-dependent values for H_i for films a–c of Fig. 8 are plotted on logarithmic axes in Fig. 10. The vertical arrows again represent the corresponding T_{c0} for each film and the right-hand axis has been converted to frequency units using Eq. (3.1) and the value $D=0.18 \text{ cm}^2\text{sec}^{-1}$. It is satisfying to note that the results for film a (squares) are not significantly different from the values obtained in an earlier analysis¹⁵ of data over a more limited field range using Larkin’s original theoretical result⁴ which includes an additional fitting parameter $\beta(T/T_{c0})$.

The solid line in Fig. 10, calculated from the relation

$$\tau_i^{-1} = \frac{k_B T}{\hbar}, \quad (4.1)$$

when evaluated at T_{c0} for each film, represents an approximate upper limit to the scattering rate which is consistent with superconductivity, i.e., where the energy broadening associated with the inelastic scattering becomes comparable to the superconducting energy gap. The MC measurements have thus confirmed that near critical disorder, where T_{c0} is decreasing rapidly with increasing R_n , the inelastic scattering rate τ_i^{-1} is near its maximum-energy-gap limited value. Furthermore, the

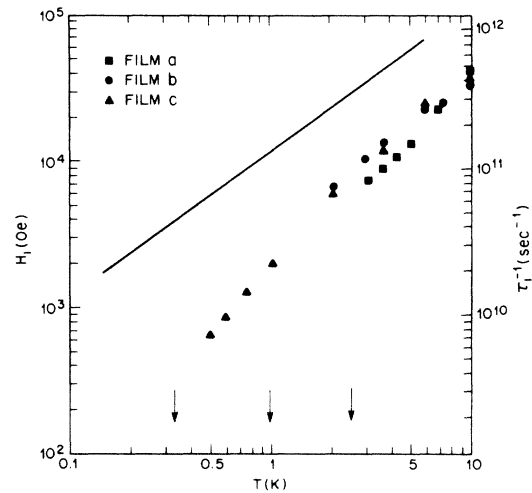


FIG. 10. Logarithmic plot of the temperature dependence of H_i (left-hand axis) and τ_i^{-1} (right-hand axis) for films a–c. The vertical arrows represent the respective transition temperatures (cf. Fig. 1) and the solid line, discussed in the text, is the approximate boundary for a scattering rate consistent with the existence of superconductivity.

approximate linear temperature dependence of τ_i^{-1} is in accord with the expected theoretical dependence of inelastic electron-electron scattering in two dimensions.^{26,28,39} The spread in values of R_n for film a (2248 Ω/\square) and film c (3454 Ω/\square) is not sufficient, however, to make a meaningful comparison with the theoretical prediction that τ_i^{-1} is proportional to R_n .

In Fig. 11 we have selected the data which has a slope closest to unity (film b of Fig. 10) and plotted in on a linear scale. The solid line represents a best fit to the expression

$$\tau_i^{-1} = \frac{k_B T}{2\epsilon_F \tau} \left[\alpha + \frac{2 \ln 2}{\ln(T/T_{c0}) + \beta} \right], \quad (4.2)$$

where $\beta = 4 \ln 2 / [(\alpha^2 + 128 \epsilon_F \tau / \pi \hbar)^{1/2} - \alpha]$, $\alpha = \ln(\epsilon_F \tau / \hbar)$, and $\epsilon_F \tau$ is the product of the Fermi energy ϵ_F and the electron scattering time τ . The first term of the above equation is the 2D normal-metal electron-electron inelastic scattering rate,²⁸ and the second term arises from the inelastic processes associated with the recombination of electrons into superconducting pairs.²² For quasi-two-dimensional films where the elastic mean free path $l \ll d$ and $L_i \gg d$, we can replace $\epsilon_F \tau$ in Eq. (4.2) by the quantity³⁹ $\pi \hbar^2 / e^2 R_n$ which thus relates τ_i^{-1} solely to R_n , the parameter which was varied in obtaining the solid-line fit of Fig. 4. The best-fit value, $R_n = 4600 \Omega/\square$, is satisfyingly close to the experimental value $R_n = 3394 \Omega/\square$. Extrapolation of the theory curve below the lowest-temperature data point shows the predicted upturn associated with the superconducting fluctuations. We emphasize, however, that there is no direct evidence of such an upturn in our data because of our inability to properly take account of the AL fluctuations for data close to T_{c0} . This is not a problem in the data of Gordon *et al.*,⁴⁰ who have observed an enhanced rate near T_{c0} in Al films with lower R_n and interpreted this enhancement using a pair-breaking rate which diverges at T_{c0} .^{41,42} It is, however, reasonable to speculate that the competition between the two different scattering processes embodied in Eq. (4.2) gives rise to an effectively temperature-independent scattering rate near $T = T_{c0}$, which thus might account for the temperature-independent pair-breaking mechanism used to describe the disorder-induced trends in T_{c0} and H_{c2} observed for similar films.¹⁵

Although the results discussed above are in good agreement with theoretical expectations and show interesting new physics for thin-film superconductors near critical disorder, it is appropriate to frame our conclusions with some cautionary remarks. The first of these is that the theory of Sec. II is a perturbative theory, valid only for $\epsilon_F \tau / \hbar \gg 1$. For film c, the most disordered film for

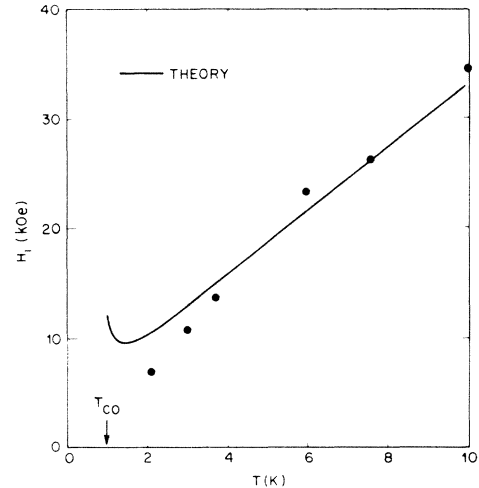


FIG. 11. Linear plot of the temperature dependence of H_i for film b. The solid line is theory.

which MC data was analyzed, $R_n = 3454 \Omega/\square$ implying $\epsilon_F \tau / \hbar = 3.7$, a number uncomfortably close to unity. The question of dimensionality is also important. For our 100-Å-thick films the dimensional crossover $d = L_i$ occurs when $H_i = \hbar c / 4e D d^2 = 16500$ Oe which from Fig. 10 is at ~ 5 K. One can argue that for this case of marginal dimensionality ($d \approx L_i$) we are unlikely to be in the 3D limit because the requisite large number of perpendicular wave vectors is not possible unless $d \gg L_i$. A similar argument can be applied to the quantum diffusion length $L_T = (\hbar D / k_B T)^{1/2}$, which for $D = 0.18 \text{ cm}^2 \text{ sec}^{-1}$ is equal to the film thickness at 1.4 K. An additional issue which has not been confronted in the analysis presented here is the magnetic field dependence of τ_i .²² Finally, in Eq. (4.2) we have chosen to use for the inelastic electron-electron scattering rate the expression given by Altschuler *et al.*²⁸ rather than the expression by Abrahams *et al.*,²⁶ which gives a factor of 5–10 greater scattering rate than that shown by the data. The theoretical issues delineating the conditions under which either one of these rates is appropriate are still unsettled.^{43,44}

ACKNOWLEDGMENTS

The authors appreciate the interest and valuable suggestions of E. Abrahams, A. T. Fiory, and J. M. B. Lopes dos Santos. We are indebted to G. A. Baraff and M. A. Marcus for helpful suggestions concerning computer coding and to H. Dail and R. H. Eick for technical assistance.

¹K. Maki, Prog. Theor. Phys. **40**, 193 (1968).

²R. S. Thompson, Phys. Rev. B **1**, 327 (1970).

³L. G. Aslamazov and A. I. Larkin, Phys. Lett. **26A**, 238 (1968).

⁴A. I. Larkin, Pis'ma Zh. Eksp. Teor. Fiz. **31**, 239 (1980) [JETP Lett. **31**, 219 (1980)].

⁵S. Maekawa and H. Fukuyama, J. Phys. Soc. Jpn. **51**, 1380 (1981).

⁶H. Takagi, R. Souda, and Y. Kuroda, Prog. Theor. Phys. **68**, 426 (1982).

⁷H. Ebisawa, S. Maekawa, and H. Fukuyama, Solid State Commun. **45**, 75 (1983).

⁸Y. Bruynseraede, M. Gijs, C. Van Haesendonck, and G. Deutscher, Phys. Rev. Lett. **50**, 277 (1983).

⁹M. B. Gershenson, V. N. Gubankov, and Y. E. Zhuralev, Solid

- State Commun. **45**, 87 (1983).
- ¹⁰P. Santhanam and D. E. Prober, *Phys. Rev. B* **29**, 3733 (1984).
- ¹¹J. M. Gordon, C. J. Lobb, and M. Tinkham, *Phys. Rev. B* **28**, 4046 (1983).
- ¹²G. Bergmann, *Phys. Rev. B* **29**, 6114 (1984).
- ¹³S. Kobayashi, S. Okuma, and F. Komori, *J. Phys. Soc. Jpn.* **52**, 20 (1983).
- ¹⁴H. Raffy, R. B. Laibowitz, P. Chaudhari, and S. Maekawa, *Phys. Rev. B* **28**, 6607 (1983).
- ¹⁵A. F. Hebard and M. A. Paalanen, *Phys. Rev. B* **30**, 4063 (1984).
- ¹⁶K. Usadel, *Z. Phys.* **227**, 268 (1969).
- ¹⁷E. Abrahams, R. Prange, and M. Stephen, *Physica (Utrecht)* **55**, 230 (1971).
- ¹⁸M. Redi, *Phys. Rev. B* **16**, 2027 (1977).
- ¹⁹B. L. Altschuler, A. G. Aronov, A. I. Larkin, and D. Khmel'nitskii, *Zh. Eksp. Teor. Fiz.* **81**, 768 (1981) [*Sov. Phys.—JETP* **54**, 411 (1981)].
- ²⁰J. M. B. Lopes dos Santos and E. Abrahams, *Phys. Rev. B* **31**, 172 (1985).
- ²¹A. T. Fiory and A. F. Hebard, *Phys. Rev. Lett.* **52**, 2057 (1984).
- ²²W. Brenig, M. Chang, E. Abrahams, and P. Wölfle, *Phys. Rev. B* **31**, 7001 (1985).
- ²³G. Baym, *Phys. Rev.* **127**, 1391 (1962).
- ²⁴W. Brenig, *J. Low Temp. Phys.* **60**, 297 (1985).
- ²⁵A. Schmid, *Z. Phys.* **271**, 251 (1974).
- ²⁶E. Abrahams, P. W. Anderson, P. A. Lee, and T. V. Ramakrishnan, *Phys. Rev. B* **24**, 6783 (1981).
- ²⁷H. Fukuyama and E. Abrahams, *Phys. Rev. B* **27**, 5976 (1983).
- ²⁸B. L. Altschuler, A. G. Aronov, and D. E. Khmel'nitskii, *J. Phys. C* **15**, 7367 (1982).
- ²⁹A. F. Hebard and S. Nakahara, *Appl. Phys. Lett.* **41**, 1130 (1980).
- ³⁰A. T. Fiory, A. F. Hebard, and W. I. Glaberson, *Phys. Rev. B* **28**, 5075 (1983).
- ³¹M. A. Paalanen and A. F. Hebard, *Appl. Phys. Lett.* **45**, 794 (1984).
- ³²G. Deutscher, H. Fenichel, M. Gershenson, E. Grünbaum, and Z. Ovadyahu, *J. Low Temp. Phys.* **10**, 231 (1973).
- ³³R. C. Dynes and J. P. Garno, *Phys. Rev. Lett.* **46**, 137 (1981).
- ³⁴A. F. Hebard and J. Vandenberg, *Phys. Rev. Lett.* **44**, 50 (1980).
- ³⁵A. F. Hebard and A. T. Fiory, *Phys. Rev. Lett.* **50**, 1603 (1983).
- ³⁶B. I. Halperin and D. R. Nelson, *J. Low Temp. Phys.* **36**, 599 (1979).
- ³⁷C. Lobb, M. Tinkham, T. M. Klapwijk, and A. D. Smith, *Physica* **107B**, 17 (1981).
- ³⁸S. Hikami, A. I. Larkin, and Y. Nagaoka, *Prog. Theor. Phys.* **63**, 707 (1980).
- ³⁹S. Maekawa, H. Ebisawa, and H. Fukuyama, *J. Phys. Soc. Jpn.* **53**, 2681 (1984).
- ⁴⁰J. M. Gordon, C. J. Lobb, and M. Tinkham, *Phys. Rev. B* **29**, 5232 (1984).
- ⁴¹B. R. Patton, *Phys. Rev. Lett.* **27**, 1273 (1971).
- ⁴²J. Keller and V. Korenman, *Phys. Rev. B* **5**, 4367 (1972).
- ⁴³H. Fukuyama, *J. Phys. Soc. Jpn.* **53**, 3299 (1984).
- ⁴⁴E. Abrahams and J. M. B. Lopes dos Santos (private communication).